Carlet, J. Clément, H. Demarne, M. Mellet, J.-P. Richaud, D. Segondy, M. Vedel, J.-P. Gagnol, R. Roncucci, B. Castro, P. Corvol, G. Evin, B. P. Roques, *ibid.* **1986**, *29*, 1152–1159; d) H. Mazdiyasni, D. B. Konopacki, D. A. Dickman, T. M. Zydowsky, *Tetrahedron Lett.* **1993**, *34*, 435–438.

[4] a) M. Frankel, P. Moses, *Tetrahedron* **1960**, *9*, 289–294; b) W. F. Gilmore, H.-J. Lin, *J. Org. Chem.* **1978**, *43*, 4535–4537; c) G. R. Moe, L. M. Sayre, P. S. Portoghese, *Tetrahedron Lett.* **1981**, *22*, 537–540; d) B. Garrigues, M. Mulliez, *Synthesis* **1988**, 810–813; e) D. Merricks, P. G. Sammes, E. R. H. Walker, K. Henrick, M. M. McPartlin, *J. Chem. Soc. Perkin Trans. 1* **1991**, 2169–2176.

[5] a) P. Garner, J. M. Park, *J. Org. Chem.* **1987**, *52*, 2361–2364; b) W. D. Lubell, H. Rapoport, *J. Am. Chem. Soc.* **1987**, *109*, 236–239; c) N. J. Miles, P. G. Sammes, P. D. Kennewell, R. Westwood, *J. Chem. Soc. Perkin Trans. 1* **1985**, 2299–2305; d) J. Jurczak, A. Golebiowski, *Chem. Rev.* **1989**, *89*, 149–164; e) M. T. Reetz, *Angew. Chem.* **1991**, *103*, 1559–1573; *Angew. Chem. Int. Ed. Engl.* **1991**, *30*, 1531–1546; f) M. T. Reetz, J. Kanand, N. Griebenow, K. Harms, *ibid.* **1992**, *104*, 1638 and **1992**, *31*, 1626–1629; g) M. R. Leanna, T. J. Sowin, H. E. Morton, *Tetrahedron Lett.* **1992**, *33*, 5029–5032.

[6] a) J. C. Carretero, L. Ghosez, *Tetrahedron Lett.* **1987**, *28*, 1101–1104; b) J. C. Carretero, M. Demillequand, L. Ghosez, *Tetrahedron* **1987**, *43*, 5125–5134; c) J. C. Carretero, J. Davies, J. Marchand-Brynaert, L. Ghosez, *Bull. Soc. Chim. Fr.* **1990**, *127*, 835–842.

[7] a) B. Musicki, T. S. Widlanski, *Tetrahedron Lett.* **1991**, *32*, 1267–1270; b) B. Musicki, T. S. Widlanski, *J. Org. Chem.* **1990**, *55*, 4231–4233; c) R. G. Henriques, T. S. Widlanski, T. Xu, J. D. Lambeth, *J. Am. Chem. Soc.* **1992**, *114*, 7311–7313; d) M. Kovacevic, Z. Brkic, Z. Mandic, M. Tomic, M. Luic, B. K. Prodic, *Croat. Chem. Acta* **1992**, *65*, 817–833.

[8] J. Huang, T. S. Widlanski, *Tetrahedron Lett.* **1992**, *33*, 2657–2660.

[9] R. C. Reynolds, P. A. Crooks, J. A. Maddry, M. S. Akhtar, J. A. Montgomery, J. A. Secrist III, *J. Org. Chem.* **1992**, *57*, 2983–2985.

[10] H. McIlwain, *J. Chem. Soc.* **1941**, 75–77.

[11] J. A. Dale, H. S. Mosher, *J. Am. Chem. Soc.* **1973**, *95*, 512–519.

[12] Starting from noncrystallized **3**, NMR analysis of the Mosher's amides revealed a ≥98:2 ratio of diastereoisomers, while starting from recrystallized **3**, the Mosher's amides were obtained as single compounds within the limits of NMR detection (>99:1).

[13] ^{13}C NMR analysis of dimers **7** revealed them to be single diastereomers.

[14] a) I. M. Gordon, H. Maskill, M. F. Ruasse, *Chem. Soc. Rev.* **1989**, *18*, 123–151; b) J. F. King, R. Rathore in *The Chemistry of Sulphonic Acids, Esters and their Derivatives* (Eds.: S. Patai, Z. Rappoport), Wiley, Chichester, **1991**, pp. 697–766.

[15] K. Hori, H. Kazuno, K. Nomura, E. Yoshii, *Tetrahedron Lett.* **1993**, *34*, 2183–2186.

[16] a) S. H. Gellman, G. P. Dado, G.-B. Liang, B. R. Adams, *J. Am. Chem. Soc.* **1991**, *113*, 1164–1173; b) G. P. Dado, S. H. Gellman, *ibid.* **1993**, *115*, 4228–4245; c) V. Dupont, A. Lecoq, J.-P. Mangeot, A. Aubry, G. Boussard, M. Marraud, *ibid.* **1993**, *115*, 8898–8906, and references therein.; d) E. A. Gallo, S. H. Gellman, *ibid.* **1993**, *115*, 9774–9788; e) G. P. Dado, S. H. Gellman, *ibid.* **1994**, *116*, 1054–1062.

[17] Usage-directed Still–Chang–Guida torsional Monte Carlo method [19a], as a part of BATCHMIN-MacroModel 3.1 molecular mechanics program [19b], was used for the conformational search on a Silicon Graphics Iris workstation. The conformers were minimized in chloroform using the GB/SA model included in BATCHMIN [19c]. MM2* parameters were used as implemented in MacroModel [19b], with the addition of suitable parameters for the sulfonamide group [19d].

[18] For a conformational analysis of vinylogous polypeptides, see: M. Hagihara, N. J. Anthony, T. J. Stout, J. Clardy, S. L. Schreiber, *J. Am. Chem. Soc.* **1992**, *114*, 6568–6570.

[19] a) G. Chang, W. C. Guida, W. C. Still, *J. Am. Chem. Soc.* **1989**, *111*, 4379–4386; b) F. Mohamadi, N. G. J. Richards, W. C. Guida, R. Liskamp, M. Lipton, C. Caufield, G. Chang, T. Hendrickson, W. C. Still, *J. Comput. Chem.* **1990**, *11*, 440–467; c) W. C. Still, A. Tempczyk, R. C. Hawley, T. Hendrickson, *J. Am. Chem. Soc.* **1990**, *112*, 6127–6129; d) L. Belvisi, O. Carugo, G. Poli, *J. Mol. Struct.* **1994**, *318*, 189–202.

Localization of Electrons in Intermetallic Phases Containing Aluminum**

Ulrich Häussermann, Steffen Wengert, Patrick Hofmann, Andreas Savin, Ove Jepsen, and Reinhard Nesper*

Dedicated to Professor Ewald Wicke on the occasion of his 80th birthday

Intermetallic phases and Zintl phases are important classes of compounds in inorganic chemistry which were for a long time considered as unusual. These compounds formed from metals, or from metals and semi-metals, possess a very large combinatorial potential, only a very small part of which has been investigated to date. Both classes demonstrate enormously varied, yet differing, aspects of structural chemistry, which are to some extent very complex. Unfortunately, the understanding of most of these structures causes great difficulties, in particular with regard to a description of their chemical bonding. These difficulties have already been reported in detail in this journal.[1]

The electron localization function (ELF) has developed into a useful tool for the interpretation of the chemical bond.[2] The ELF is particularly attractive for crystalline materials, because it is not wave vector dependent and, like electron density, is only a function of the three positional coordinates (x,y,z). Originally derived from the Hartree–Fock pair density for electrons with the same spin by Becke and Edgecombe,[3] it is a measure of the probability of finding an electron in the surroundings of another electron with the same spin. The ELF is normalized so that its dimensionless values lie between zero and one. Large values correspond to a high localization and mean that for an electron with a particular spin, located at (x,y,z), no other electron with the same spin is to be found in the vicinity. Such a situation may also be interpreted as meaning that an electron pair with α,β spin is localized in the region around (x,y,z).[4] This interesting result, that the probability of finding an electron pair is dependent on the location, is based entirely on the Fermi correlation. The Coulomb correlation, which opposes the formation of an electron pair, is not taken into consideration in the calculation of the ELF. High ELF values have indeed been found for those regions which correspond to bonds, lone pairs of electrons, and electron shells.

The term localization, in the sense of the ELF, describes thus the tendency of formation of electron pairs at a position (x,y,z), whereas the electron density $\rho(x,y,z)$ is the probability density for an electron in an arbitrary spin state at this position. The value ELF = 0.5 represents the situation in an homogeneous electron gas, a model system without atomic cores, which serves as a reference. The deviations from this value are caused by the presence of the atomic cores, that is, by the formation of a structure. As a result of these, domains of high localization are

[*] Prof. Dr. R. Nesper, Dipl.-Chem. U. Häussermann, Dipl.-Chem. S. Wengert, Dipl.-Chem. P. Hofmann
Laboratorium für Anorganische Chemie der Eidgenössischen Technischen Hochschule
Universitätstrasse 6, CH-8092 Zürich (Switzerland)
Telefax: Int. code + (1)632-1149

Priv.-Doz. Dr. A. Savin
CNRS, Laboratoire Dynamique des Interactions Moleculaires
Université Pierre et Marie Curie, Paris (France)

Dr. O. Jepsen
Max-Planck-Institut für Festkörperforschung, Stuttgart (FRG)

[**] This work was supported by the Schweizerische Nationalfonds zur Förderung der wissenschaftlichen Forschung.

formed, for example, in bonds, and domains of low localization, for example, between the electron shells in atoms.

In the meantime, the ELF has also been calculated by using density matrices from density functional methods[5] and even by using those from semiempirical calculations.[6] Strictly speaking, the interpretation given above does not hold for these procedures. In spite of this, the results correspond to a great extent, and we would like therefore to use our interpretation, independent of the method of calculation employed.[7]

Both the electron density and the ELF values are shown in the two-dimensional graphical representation. The electron densities are displayed as point densities and the corresponding ELF values coded in the form of a color scale, similar to that used in a map. High ELF values (ca. 0.8–1.0) are colored white; the series descends through brown and yellow to green for middle ELF values (ca. 0.5); blue and violet then indicating the lower end of the scale.[8]

The abrupt transition within the third period from the metallic bond in aluminum to the covalent bond in silicon can take place in a stepwise manner in intermetallic compounds and Zintl phases containing aluminum. This will be demonstrated using the series $Al \rightarrow CaAl_2 \rightarrow SrAl_2 \rightarrow BaAl_4 \rightarrow CaAl_2Si_2 \rightarrow Si$ as an example.[9]

The structure of elemental aluminum is a cubic close packed arrangement (fcc, Fig. 1a). Each Al atom has twelve nearest

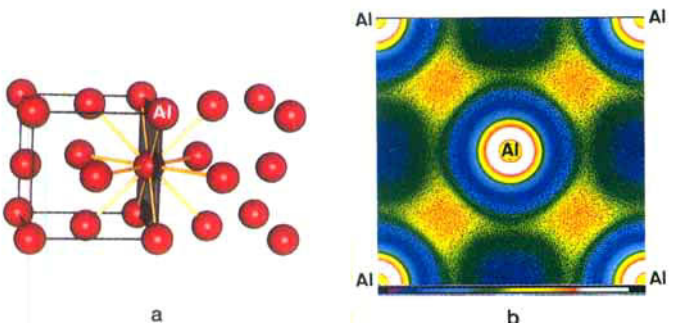

Fig. 1. a) Section from the fcc structure of aluminum showing the (100) plane and connecting lines to the twelve nearest neighbors (yellow). The edges of the unit cell are indicated by black lines in all structure diagrams. b) Electron density ρ (density of points) and ELF (color) for the (100) plane in Al. The ELF color scale is shown at the lower edge of the picture (see text). The electron shells of the cores cannot be entirely resolved in these diagrams, especially those of the heavier elements.

neighbors at a distance of 286.3 pm which form a cuboctahedral coordination. The ELF was calculated for the (100) plane (Fig. 1b). Clearly, the brown areas of highest localization can be recognized between nearest neighboring nuclei and the blue regions of lowest localization in the empty octahedral holes of the structure. The difference between the electron densities at these positions is approximately 100%, the ELF values, however, vary between 0.21 and 0.62, and clearly show that an electron-gas-like localization, which may perhaps have been expected, does not exist in elemental aluminum.

$CaAl_2$ crystallizes in the $MgCu_2$ structure (Fig. 2a) and thus belongs to the cubic Laves phases. All the Al atoms are symmetry-equivalent and connected to give a three-dimensional network of corner-sharing tetrahedra. Thus, each Al atom has six equivalent nearest neighbors at a distance of 284.2 pm. The Ca partial structure is diamond-like. If the twelve Al atoms at a distance of 333.2 pm are taken into consideration, the coordination polyhedron for Ca is a Friauf polyhedron (coordination number 16). The (110) plane contains zigzag chains of Ca atoms and bisects the Al_4 tetrahedra (cf. Fig. 2a). Regions with high ELF values are not only to be found between Al cores, but also extend between Al and Ca cores. The maximum ELF values are 0.74 (Fig. 2b). All tetrahedral faces lie in the (111) planes and

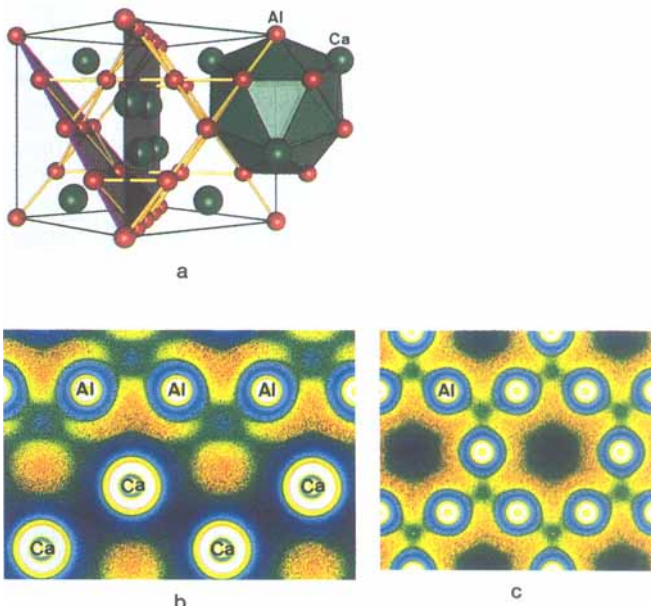

Fig. 2. a) Section from the cubic $CaAl_2$ structure (Ca: green; Al: red; edges of the Al_4 tetrahedra: yellow; coordination polyhedra of Ca: green) showing the (111) (violet border) and (110) planes (black border). b) ρ and ELF for the (110) plane in $CaAl_2$. c) ρ and ELF for the (111) plane in $CaAl_2$.

the corresponding Al atoms form the Kagomé net, a connection pattern comprising equal numbers of triangles and hexagons (3636 net, Fig. 2c). In the tetrahedral faces, green regions of electron-gas-like behavior is found. The localization in the middle of the hexagons is the lowest for the valence region (ELF = 0.115). The ELF values in $CaAl_2$ are admittedly higher than in metallic Al, they are, however, too small for usual covalent bonds. The structure of the localization pattern resembles that of banana bonds.

Figure 3a shows the $SrAl_2$ structure ($CeCu_2$ type) in which the Al atoms form slightly puckered nets of hexagonal rings stacked in the [100] direction. The Al–Al distances in the net are 278.6 and 279.9 pm. Longer bonds (293.0 pm) connect these nets through chains of four-membered rings which follow the [010] direction. All in all, the Al coordination polyhedron is a slightly distorted trigonal pyramid. The Sr atoms are located between the nets of six-membered rings and are coordinated by twelve Al atoms. The (040) plane cuts perpendicularly through the stacked nets of hexagonal rings. The Sr atoms, one sort of Al–Al bond in the nets (279.9 pm), and the long bonds connecting the nets all lie in this plane. The electron density distribution and the ELF for this plane are shown in Figure 3b. White regions can be distinguished between the Al cores, that is, regions of high ELF, which indicate a bonding electron pair. Figure 3c shows the localization behavior in one of the four-membered Al rings. In contrast to $CaAl_2$ (Fig. 2), the areas of highest localization in $SrAl_2$, with maximum ELF values of around 0.88, are entirely due to the Al partial structure, which can be described as a covalent network.

In the $BaAl_4$ structure, one sort of Al atom, which may be described as basal, forms a quadratic net with large Al–Al

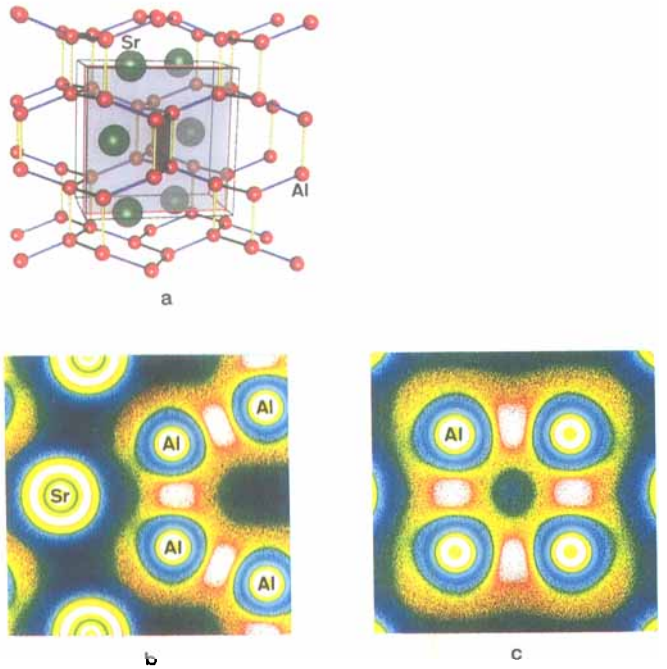

Fig. 3. a) Section from the $SrAl_2$ structure (Sr: green; Al: red). The Al–Al bonds forming the nets of hexagonal rings are colored blue and those connecting the nets yellow. The (040) plane is colored violet. Additionally, a four-membered Al ring from one of the chains of four-membered rings in the [010] direction is shaded for emphasis. b) ρ and ELF for the (040) plane in $SrAl_2$. c) ρ and ELF for a four-membered Al ring in $SrAl_2$.

distances of 321.0 pm (Fig. 4a). The squares are alternately capped from above and below by the second sort of Al atom, the apical ones, to form pyramids. In addition, these apical Al atoms connect the pyramid layers so that the tips of neighboring

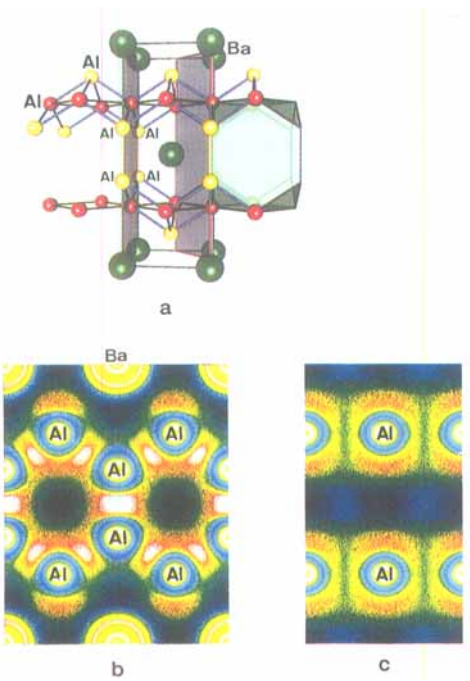

Fig. 4. a) Section from the $BaAl_4$ structure (Ba: green; apical Al: yellow; basal Al: red; coordination polyhedron of Ba: green). The (220) plane (red-violet border) contains the distances between the basal Al atoms (black rods), the (110) plane contains the bonds between the basal and the apical Al atoms (blue rods), and those between the apical Al atoms (yellow rods). b) ρ and ELF for the (100) plane in $BaAl_4$ (2 unit cells). c) ρ and ELF for the (220) plane in $BaAl_4$ (2 unit cells).

layers lie directly above one another. Each of the Ba atoms is situated in one of the large cavities between the layers and is coordinated by 16 Al atoms. The bonding in the Al framework was interpreted as follows:[10] The distance of 278.4 pm between the apical Al atoms represents a two-electron, two-center (2e–2c) bond; 6e–5c bonds are found between the apical and the basal Al atoms, although the distance is somewhat shorter (272.5 pm). The two types of bonds lie in the (100) plane, for which the electron density distribution and ELF are shown in Figure 4b and can be distinctly differentiated in this case. The larger white regions, with a maximum ELF value of 0.93 between the apical Al atoms, correspond to the electron pairs of the 2e–2c bonds. The smaller white regions between the apical and the basal Al atoms are attributed to multicenter bonds (highest localization value ca. = 0.85). The long Al–Al distances of the quadratic net lie in the (220) plane. The ELF runs through a minimum between these atoms, which can clearly be recognized by the green areas between the basal Al atoms, and which excludes the possibility of a bonding interaction (Fig. 4c). It is this conclusion which allows for the formulation of the 6e–5c bond as such.

Figure 5a shows the structure of $CaAl_2Si_2$. Al atoms and Si atoms form puckered double layers of hexagonal rings. Al and Si atoms are alternately arranged in a net of hexagonal rings at distances of 248.9 pm. The longer Al–Si bonds of 257.2 pm

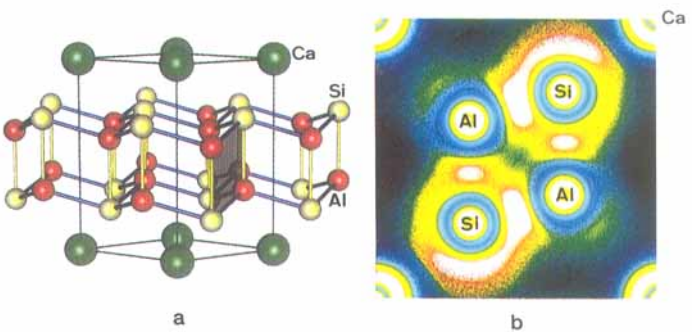

Fig. 5. a) Section from the hexagonal $CaAl_2Si_2$ structure (Ca: green; Al: red; Si: yellow). The short Al–Si distances in a layer of hexagonal rings are colored blue-violet, the long distances connecting the layers colored yellow. The central building block of the double layer, the oblique Al_2Si_2 four-membered ring, is shaded for emphasis. b) ρ and ELF for the (120) plane in $CaAl_2Si_2$. The section shows the Ca nuclei in the corners and an Al_2Si_2 four-membered ring.

connect to form a double layer. The Si atoms in a double layer always occupy the peripheral positions and are rather strangely coordinated by four Al atoms, somewhat resembling an umbrella, whereas the Al atoms are surrounded tetrahedrally by four Si atoms. The Ca atoms are located between the double layers in the middle of two six-membered rings. The (120) plane contains the central building unit of the double layer, an Al_2Si_2 four-membered ring with one long and three short Al–Si bonds. The ELF permits the recognition of a lone electron pair on the Si atom (maximum ELF value = 0.86 for this region). The highest localization values in the valence area of this compound (ca. 0.91), however, are found along the short Si–Al bond (Fig. 5b). This bond, like the longer Si–Al bond connecting the layers, is clearly polarized in the direction of the somewhat more electronegative Si atoms, the maximum ELF value lying at 0.84. The semi shell-shaped distribution of the high ELF values around Si indicates an intermediate state between the purely covalent and ionic situations represented by the formulas

  0570-0833/94/2020-2071 $ 10.00+.25/0

$Ca^{2+}(Al^{3+})_2(Si^{4-})_2$ and $Ca^{2+}(4b)[AlSi]^{2-}$.[*] A bonding interaction between Al atoms, as had been assumed in the literature,[11] cannot be recognized.

Silicon in the diamond structure (Fig. 6a) does of course have extended regions of high localization between the nuclei, where the bonding electron pairs are situated. Figure 6b shows the (110) plane. The large differences in the electron densities in the valence region are quite remarkable. Very little electron density (black areas) is found between the zigzag chains in comparison to that located in the regions between the cores, where the highest localization values (ELF = 0.95) are found.

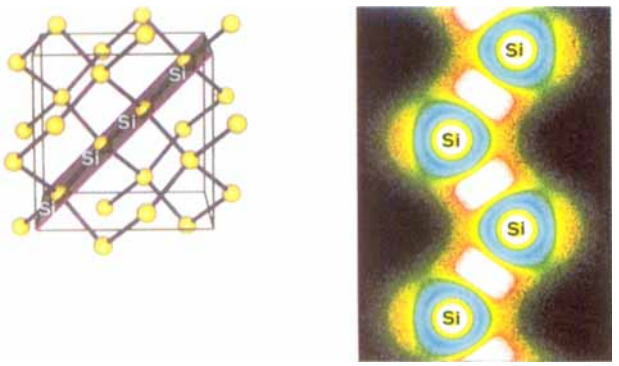

Fig. 6. a) Diamond structure showing the (110) plane. b) ρ and ELF for the (110) plane in α-Si.

Structures with large differences in electron density in the valence regions are normally divided into covalent and ionic structures. In contrast, intermetallic phases have a more uniform density distribution. In spite of this, our ELF results demonstrate that both bonding electron pairs and lone pairs do occur in these compounds, just as in the covalent and ionic structures which are understood in terms of the valence rules. For those compounds in which the chemical bond is described as a metallic bond (fcc Al and $CaAl_2$), the occurrence of numerous ELF maxima (with respect to the number of valence electrons in the unit cell) is characteristic; however, the absolute value of these does not usually exceed 0.75. The number and the position of these maxima can vary to a great extent within a simple structural type.[14] In structures with localized multicentered bonds (6e–5c bond within Al_5 pyramids in $BaAl_4$), the maximum ELF values lie above 0.8 in the regions of these bonds. For bonding electron pairs, maximum ELF values of about 0.9 are to be expected, whereas for lone pairs somewhat smaller values are found.

This relationship is further clarified in the Figures 7a–7d, in which the electron density (dotted line) and the ELF (full line) along symmetrical bonds are plotted in a one-dimensional representation. The shell structure of the cores is easily discernible. Figure 7a shows the Al–Al bond in fcc aluminum and Figure 7b the 2e–2c bond between the apical Al atoms in $BaAl_4$. The electron density difference in the middle of the bond amounts to only about 20%, but the ELF shows impressively the difference between the chemical bonds for the two Al pairs. The course of the ELF along the 2e–2c Al–Al bond is the same as that for the Si–Si bond in α-Si (Fig. 7c). The electron density in the middle of the Si–Si bond, however, is more than twice as large as that in the Al–Al bond. Finally, the situation for the large distance between the basal Al atoms in the $BaAl_4$ structure is shown in Figure 7d. The ELF minimum observed between these cores clearly shows the nonbonding character.

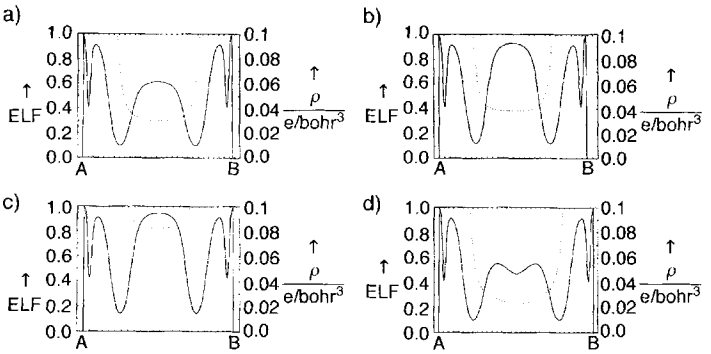

Fig. 7. ρ (dotted line) and ELF (full line) a) along the Al–Al bond in fcc aluminum, b) along the 2e-2c bond between the apical Al atoms in $BaAl_4$, c) along the Si–Si bond in α-Si, d) along the distance between basal atoms in $BaAl_4$. The atoms involved in a particular bond are labeled A and B accordingly.

This discussion sheds new light on the problem of the interpretation of bond lengths in intermetallic phases: In $BaAl_4$, for example, the Al–Al distance, which is attributed to the 6e–5c bond, is about 6 pm shorter than the 2e–2c bond—contrary to expectations when bond lengths and bond orders are correlated with one another! Similarly, a bond order of around one has to be attributed to the Al–Al distance of 293 pm in $SrAl_2$, although this distance is considerably larger than the Al–Al distance in the metal (286.3 pm) with a bond order of 0.25. In our opinion, a simple relationship between bond length and bond strength[12] or bond order[13] does not exist in the compounds discussed here. In contrast, the ELF can be of decisive assistance in the classification of the diverse interatomic vectors in intermetallic compounds.

New approaches for a more quantitative interpretation of ELF results are being made by using a topological analysis of the ELF (x,y,z) scalar field. The unequivocal attribution of the numbers of electrons to the ELF maxima, described as localization attractors,[15] as well as the possibility of defining a scale of ionic character[16] must be mentioned at this point.

Received: March 19, 1994 [Z6778IE]
German version: *Angew. Chem.* **1994**, *106*, 2147

[*] $(4b)[AlSi]^{2-}$ refers to a four-bonded framework made of Si and Al in which each atom is assigned four valence electrons.

[1] R. Nesper, *Angew. Chem.* **1991**, *103*, 805; *Angew. Chem. Int. Ed. Engl.* **1991**, *30*, 789.
[2] A. Savin, A. D. Becke, J. Flad, R. Nesper, H. Preuß, H. G. von Schnering, *Angew. Chem.* **1991**, *103*, 421; *Angew. Chem. Int. Ed. Engl.* **1991**, *30*, 409.
[3] A. D. Becke, K. E. Edgecombe, *J. Chem. Phys.* **1990**, *92*, 5397.
[4] R. F. W. Bader, *Atoms in Molecules: A Quantum Theory*, Clarendon, Oxford, **1990**.
[5] A. Savin, O. Jepsen, J. Flad, O. K. Andersen, H. Preuß, H. G. von Schnering, *Angew. Chem.* **1992**, *104*, 186; *Angew. Chem. Int. Ed. Engl.* **1992**, *31*, 187.
[6] A. Burkhard, U. Wedig, H. G. von Schnering, A. Savin, *Z. Anorg. Allg. Chem.* **1993**, *619*, 437.
[7] A different interpretation of ELF is given by A. Savin et al. in [5].
[8] J. Flad, F.-X. Fraschio, B. Miehlich, Programm GRAPA, Institut für Theoretische Chemie der Universität Stuttgart, **1989**.
[9] All structural data taken from P. Villars, L. D. Calvert, *Pearson's Handbook of Crystallographic Data for Intermetallic Phases*, 2nd ed., ASM International, OH, USA, **1991**. Electron density distribution and ELF values calculated using the LMTO method (LMTO = linear muffin tin orbital): M. van Schilfgaarde, T. A. Paxton, O. Jepsen, O. K. Andersen, Program TB-LMTO. Empty spheres at the position $(0.0,\frac{1}{2})$ in the $CaAl_2Si_2$ structure (in the middle of the double layer, Ca at (0,0,0)) and at the site $(\frac{1}{2},\frac{1}{2},\frac{1}{2})$ in the Si–diamond structure (Si at (0,0,0)). The sizes of the muffin-tin spheres were chosen so that the best possible compromise between space-filling and overlap was achieved.

[10] C. Zheng, R. Hoffmann, *Z. Naturforsch. B* **1986**, *41*, 292.
[11] C. Zheng, R. Hoffmann, R. Nesper, H. G. von Schnering, *J. Am. Chem. Soc.* **1986**, *108*, 1876.
[12] L. Pauling, *The Nature of the Chemical Bond*, Cornell University Press, Ithaca, NY, **1960**; *Die Natur der chemischen Bindung*, Verlag Chemie, Weinheim, **1976**.
[13] M. O'Keefe in *Modern Aspects in Inorganic Crystal Chemistry* (*NATO ASI Ser. C* **1992**, *382*, S. 163.
[14] In fcc Ca, the maximum ELF values lie close to the octahedral holes.
[15] U. Häußermann, S. Wengert, R. Nesper, *Angew. Chem.* **1994**, *106*, 2150; *Angew. Chem. Int. Ed. Engl.* **1994**, *33*, 2073.
[16] B. Silvi, A. Savin, unpublished results.

Unequivocal Partitioning of Crystal Structures, Exemplified by Intermetallic Phases Containing Aluminum**

Ulrich Häussermann, Steffen Wengert, and Reinhard Nesper*

Dedicated to Professor Ewald Wicke on the occasion of his 80th birthday

Crystal chemical parameters, such as partial volumes,[1] partial charges,[2] bond strengths,[3] and coordination numbers[4] have long been successfully employed in crystal structure analysis to understand and to interpret structures. There have always been attempts to define such incremental parameters as unequivocally as possible. In this context, the partitioning of space in a crystal structure into domains of its building blocks[***][5] is a useful approach and delivers important information about the parameters mentioned above.

Using the ordering of spheres of equal size as an example, Niggli introduced the concept of the "Wirkungsbereich" as far back as 1927.[5] According to his definition, the Wirkungsbereich of a sphere comprises all points in space whose distances from the sphere are smaller than those to all other spheres. The simplest polyhedron marking this domain is constructed with perpendicular planes at the midpoints of the lines connecting neighboring spheres. When the hypothetical spheres, that is, the atoms or ions, have different radii, the connecting lines can be divided according to the ratio of the radii. In many cases this procedure does, however, lead to polyhedra that are not totally space-filling. The construction procedure developed by Fischer, Koch, and Hellner yields better results.[6] Here, the division of the connecting lines between neighboring spheres by means of the exponential plane construction guarantees that no gaps occur in the partitioning of space and always leads to a convex polyhedron for every occupied point position of the crystal structure. However, this method too is still dependent on the choice of radii for the spheres, that is, on the definition of atomic or ionic radii.[7]

According to Bader,[8] a clear partitioning of the three-dimensional space into atomic domains can be achieved by the analysis of the scalar field, the electron density $\rho(x,y,z)$, and the gradient $\Delta\rho(x,y,z)$. The (3,−1) saddle points[9] of the electron density play an important role here. The sum of all the trajectories[10] that end on these saddle points form surfaces in three-dimensional space, which define the atomic boundary. In crystalline structures, these surfaces form closed polyhedra around the atomic nuclei. The polyhedra fill the volume of the unit cell completely[*] and thus provide the best definition for atomic domains. In addition, the faces of the polyhedra fulfill the conditions for a vanishing density flow, that is, $\Delta\rho(x,y,z)\vec{n}(x,y,z) = 0$ for all points (x,y,z) on these faces, where $\vec{n}(x,y,z)$ is the unit vector perpendicular to the face.

The use of the scalar field, electron localization function (ELF),[11] also leads to an unequivocal partitioning of three-dimensional space. We will designate the resulting fragments as domains of electrons and atomic cores. The regions of space occupied by bonding electrons or lone pairs are examples of domains of valence electrons. Their centers correspond to the local ELF maxima ((3,−3) points) in the valence region. The positions of the nuclei also correspond to local maxima defined by the first electron shell. The other electron shells of the core are, however, not resolved, and the ELF minimum of the outermost filled shell is thus used to specify the domain of an atomic core. The sum of these domains once again fills the unit cell completely.

The boundaries of the domains can be used as limits of integration for the following volume integrals:

a) Volume of domain A: $V_A = \int_{V_A} dV$

b) Number of electrons in this domain A: $N_A = \int_{V_A} \rho(x,y,z)dV$

The volume and the corresponding number of electrons are important characteristic parameters of such a domain or Wirkungsbereich. In addition, the net charge of an atom can be calculated from the corresponding number of electrons of an atomic domain.[12]

There is of course a close relationship between the volume of an atomic domain and the number of electrons. This was recognized by Biltz as far back as 1934.[1] The analysis of the empirically determined domain volumes (volume increments) in a large number of compounds showed that these volumes depend to a large extent on the environment, that is, on the bonding character of the atoms in the structure. In addition to such local influences, Biltz was also able to confirm relationships between the core potentials and the volume requirement of the corresponding valence electrons. This allowed him to define volume increments for three main classes of compounds.

Based on Bader's definition of the domain of an atom, interesting relationships between chemical bonding, volume, and number of electrons can be clearly quantified. This is especially true for changes in these quantities with the formation of a compound. The domain of electrons based on the ELF can be used for the analysis of chemical bonding. Moreover, the volumes and the shapes of both types of domains contain important chemical information relevant to the structure. Based on the example of the series Al, $CaAl_2$, $SrAl_2$, $BaAl_4$, $CaAl_2Si_2$, and Si in which a transition from metallic to covalent bonding occurs,[13] these distinct possibilities of spatial partitioning will be described.[14]

Figure 1a (top) shows the contour diagram of the electron density for face-centerd cubic (fcc) aluminum in the (100) plane. The (3,−1) saddle points lie exactly at the midpoint between neighboring nuclei. The trajectories defining the atomic domains begin at the local density minima of the octahedral holes (edges of the unit cell) and end at the (3,−1) saddle points. In

[*] Prof. Dr. R. Nesper, Dipl.-Chem. U. Häussermann, Dipl.-Chem. S. Wengert
Laboratorium für Anorganische Chemie der Eidgenössischen Technischen Hochschule
Universitätstrasse 6, CH-8092 Zurich (Switzerland)
Telefax: Int. code + (1)632-1149

[**] This work was supported by the Schweizerische Nationalfonds zur Förderung der wissenschaftlichen Forschung.

[***] Also known as Wirkungsbereiche or Dirichlet domain.

[*] A requirement is that the nuclear positions are the sole electron density maxima. This is usually the case [8].

  0570-0833/94/2020-2073 $ 10.00+.25/0